Available online at www.sciencedirect.com
ScienceDirect
Journal of Sound and Vibration 297 (2006) 823–841
JOURNAL OF SOUND AND VIBRATION
www.elsevier.com/locate/jsvi

Flexural free vibration of sandwich flat panels with laminated anisotropic face sheets

Terry Hause[a,*], Liviu Librescu[b]

[a]*Mechanical and Civil Engineering, Minnesota State University at Mankato, Mankato, MN 56001, USA*
[b]*Engineering Science and Mechanics, Virginia Polytechnic Institute & State University, Blacksburg, VA 24061-0219, USA*

Received 5 April 2005; received in revised form 25 April 2006; accepted 26 April 2006
Available online 27 July 2006

Abstract

A study of the effects of anisotropy of face sheets, of core layer, and as of other mechanical/geometrical parameters of flat sandwich panels on their eigenfrequency characteristics is presented. The study is carried out in the context of an advanced model of sandwich structures featuring monoclinic anisotropy-type laminated face sheets and an orthotropic light core. A detailed analysis of the influence of a number of important parameters associated with panel geometry, fiber orientation and stacking sequence in the face sheets, and material properties of the core is carried out, and pertinent conclusions are outlined. In spite of the intricacy of the investigated problem, the adopted solution methodology of the problem enables one to obtain a closed-form solution of eigenfrequency predictions. Numerical simulations highlighting the implications of a number of parameters on eigenfrequencies, as well as validations against the few ones available in the specialized literature, are presented. Pertinent conclusions regarding their dynamic optimization via the use of directional properties of fiber-composite materials in the face sheets and of orthotropicity in the core layer material are supplied.

1. Introduction

A renewed interest for the use of sandwich structures in the construction of advanced supersonic/hypersonic flight vehicles, reusable space transportation systems, and naval ships and submarine structures has been manifested in the last decade. Some of the underlying reasons and motivation for this interest emerge, among others, from (1) the possibility to integrate advanced fiber-reinforced composite materials in face sheets and the core, their use being likely to provide increased bending stiffness without weight penalties, long fatigue life, directional properties, as well as the capability of operating in a high-temperature environment, (2) the possibility of providing sound insulation as well as a smooth aerodynamic surface in a higher speed flow environment, and (3) extended operational life as compared to stiffened-reinforced structures that are weakened by the appearance of stress concentration. Needless to say, the development of new manufacturing techniques that make the use of sandwich structures economically feasible has contributed greatly to the widespread use of such structures in the aerospace and marine industries.

*Corresponding author.
E-mail address: terry.hause@mnsu.edu (T. Hause).

0022-460X/$ - see front matter © 2006 Elsevier Ltd. All rights reserved.
doi:10.1016/j.jsv.2006.04.024

One of the problems related to *advanced* sandwich constructions that, in spite of its importance, has not yet received the attention it deserves is that of their free vibration (see, in this sense, the most recent survey papers and monographs on sandwich structures [1–6] as well as the study in Ref. [7]). Indeed, a good understanding of the free vibration behavior of such structures is essential toward a reliable prediction of their dynamic response to time-dependent external excitations, prevention of the occurrence of the resonance, evaluation of their flutter instability, and toward their optimal design from the vibrational point of view. This study, which is devoted to the free vibration problem of flat anisotropic sandwich panels, is intended to fill the existing gap in the specialized literature. Interested readers who want to gain a perspective of this general area are referred to Refs. [8a,b; 9].

2. Basic assumptions

The global middle plane of the sandwich structure σ, selected to coincide with that of the core layer, is referred to a curvilinear and orthogonal coordinate system x_α ($\alpha = 1, 2$). The through-the-thickness coordinate x_3 is considered positive when measured in the direction of the downward normal (see Fig. 1). For the sake of convenience, the quantities affiliated with the core layer are identified by a superposed bar, while those associated with the bottom and top face sheets are identified by single and double primes, respectively. Consistent with this convention, the uniform thickness of the core is denoted as $2\overline{h}$, and those of the upper and bottom face sheets as h'' and h', respectively. As a result, the total thickness of the structure (see Fig. 1), and the total thickness of the top and bottom face sheets are defined as

$$H = 2\overline{h} + h' + h'' \quad \text{and} \quad \hat{h} = h' + h''. \tag{1a,b}$$

In developing the theory of flat sandwich panels, the following assumptions are adopted: (i) the face sheets are laminated from orthotropic material laminae, the axes of orthotropy of the individual plies being rotated with respect to the geometrical axes x_α of the structure by the angle θ referred to as the ply-angle; in this way, the material of each layer of face sheets exhibits anisotropy of the monoclinic type; (ii) the material of the core layer features orthotropic properties in the transverse shear directions, (x_α, x_3); (iii) the core layer is capable of carrying transverse shear stresses only, and as a result we deal with a *weak core*; (iv) a perfect bonding between the face sheets and the core, and between the constituent laminae of the face sheets is postulated; (v) the assumption of core inextensibility in the transverse normal direction is adopted; (vi) the faces are assumed to be thin, and as a result transverse shear effects are neglected in the face sheets; (vii) the structure as a whole, as well as both the top and bottom laminated face sheets are assumed to exhibit mechanical and geometrical symmetry properties with respect to both the mid-plane of the core layer, and about their own mid-planes.

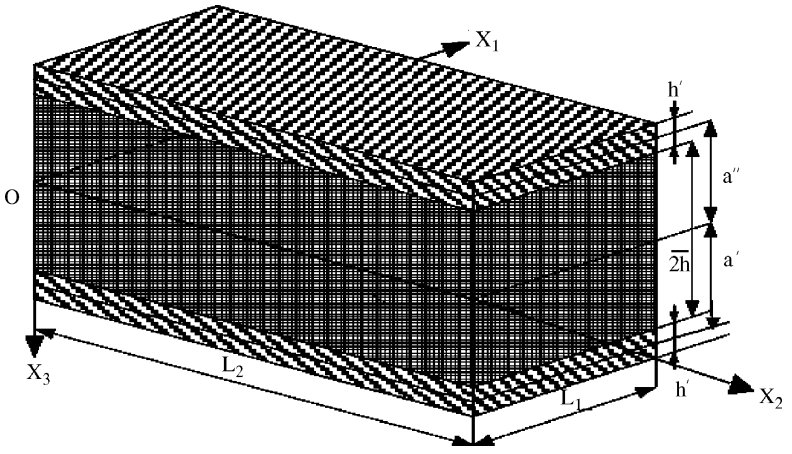

Fig. 1. Geometry of the sandwich flat panel.

3. Kinematics

3.1. The 3-D displacement field in the face sheets and the core

In agreement with the previously stipulated assumptions, the transverse displacement should be uniform through the thickness of the laminate, thus implying

$$V'_3(x_1,x_2,x_3,t)=V''_3(x_1,x_2,x_3,t)=\overline{V}_3(x_1,x_2,x_3,t)\equiv v_3(x_1,x_2,t)=v_3(x_\alpha,t). \tag{2}$$

Based on statement (vi) indicated in the previous section, the 3-D distribution of the displacement field in the face sheets and the core layer, fulfilling the interface kinematic continuity conditions, is follows [4,10–12].

In the bottom face sheets:

$$V'_1(x_\alpha,x_3,t)=\xi_1(x_\alpha,t)+\eta_1(x_\alpha,t)-(x_3-a)\frac{\partial v_3}{\partial x_1}, \tag{3a}$$

$$V'_2(x_\alpha,x_3,t)=\xi_2(x_\alpha,t)+\eta_2(x_\alpha,t)-(x_3-a)\frac{\partial v_3}{\partial x_2}\quad(\overline{h}\leqslant x_3\leqslant\overline{h}+h'), \tag{3b}$$

$$V'_3(x_\alpha,x_3,t)=v_3(x_\alpha,t). \tag{3c}$$

In the core:

$$\overline{V}_1(x_\alpha,x_3,t)=\xi_1(x_\alpha,t)+(x_3/\overline{h})\left\{\eta_1(x_\alpha,t)+(h/2)\frac{\partial v_3}{\partial x_1}\right\}, \tag{4a}$$

$$\overline{V}_2(x_\alpha,x_3,t)=\xi_2(x_\alpha,t)+(x_3/\overline{h})\left\{\eta_2(x_\alpha,t)+(h/2)\frac{\partial v_3}{\partial x_2}\right\}\quad(-\overline{h}\leqslant x_3\leqslant\overline{h}), \tag{4b}$$

$$\overline{V}_3(x_\alpha,x_3,t)=v_3(x_\alpha,t). \tag{4c}$$

In the top face sheets:

$$V''_1(x_\alpha,x_3,t)=\xi_1(x_\alpha,t)-\eta_1(x_\alpha,t)-(x_3+a)\frac{\partial v_3}{\partial x_1}, \tag{5a}$$

$$V''_2(x_\alpha,x_3,t)=\xi_2(x_2,t)-\eta_2(x_\alpha,t)-(x_3+a)\frac{\partial v_3}{\partial x_2}\quad(-\overline{h}-h''\leqslant x_3\leqslant-\overline{h}), \tag{5b}$$

$$V''_3(x_\alpha,x_3,t)=v_3(x_\alpha,t). \tag{5c}$$

In these equations, $V_i(x_\alpha,x_3,t)$ are the 3-D displacement components in the direction of coordinate x_i, while $\xi_\alpha(x_\omega,t)$ and $\eta_\alpha(x_\omega,t)$ that are defined as

$$\xi_\alpha=(\mathring{V}'_\alpha+\mathring{V}''_\alpha)/2,\quad \eta_\alpha=(\mathring{V}'_\alpha-\mathring{V}''_\alpha)/2 \tag{6a,b}$$

denote the 2-D tangential average in-plane and half-difference of in-plane displacements, respectively, where $\mathring{V}'_\alpha$ and $\mathring{V}''_\alpha$ stand for the in-plane displacements of the points of the mid-planes of the bottom and top face sheets, respectively.

For a symmetric sandwich panel, $h'=h''\equiv h$ define the thickness of the bottom and top face sheets, while $a'=a''=a(\equiv\overline{h}+h/2)$ are the distances between the global mid-plane of the structure and the mid-planes of the bottom and top face sheets, respectively. For the case considered here, these distances are equal. In the previous and next equations, Greek indices have the range 1, 2 while Latin indices have the range 1, 2, 3, and unless otherwise stated, the Einstein summation convention over the repeated indices is employed.

One of the goals of this paper is to address the problem of determination of eigenfrequencies in the context of this rather comprehensive structural model of flat sandwich structures that incorporates the directional property of the materials of face sheets. In particular, as will be highlighted in numerical simulations, this property of fibrous composites can be used to enhance the free vibrational behavior of these structures.

To be reasonably self-contained, in the following sections, the basic equations of sandwich plate theory incorporating the anisotropy of the individual face sheets and transverse shear effects in the core layer are displayed only to the extent that they are needed in the treatment of the subject considered in this paper. For more details related to the derivation of pertinent equations, the reader is referred to papers [4,10–13] where only static problems have been studied.

3.2. Distribution of strains across the thickness of the sandwich panel

Based on the representation of the displacement field, Eqs. (3)–(5),, the components of the 3-D strain tensor e_{ij} are as follows.

In the bottom face sheets:

$$e'_{11} = \varepsilon'_{11} + (x_3 - a)\kappa'_{11}, \tag{7a}$$

$$e'_{22} = \varepsilon'_{22} + (x_3 - a)\kappa'_{22}, \tag{7b}$$

$$2e'_{12} = \gamma'_{12} + (x_3 - a)\kappa'_{12}, \tag{7c}$$

In the weak core layer:

$$2\overline{e}_{13} = \overline{\gamma}_{13}, \quad 2\overline{e}_{23} = \overline{\gamma}_{23}, \tag{8a,b}$$

In the top face sheets:

$$e''_{11} = \varepsilon''_{11} + (x_3 + a)\kappa''_{11}, \tag{9a}$$

$$e''_{22} = \varepsilon''_{22} + (x_3 + a)\kappa''_{22}, \tag{9b}$$

$$2e''_{12} = \gamma''_{12} + (x_3 + a'')\kappa''_{12}. \tag{9c}$$

In these equations ε_{11}, ε_{22}, ε_{12} ($\equiv \gamma_{12}/2$) and ε_{13} ($\equiv \gamma_{13}/2$), ε_{23} ($\equiv \gamma_{23}/2$) denote the 2-D strain measures. Expressions in terms of the 2-D displacement quantities are provided in the appendix.

4. Equations of motion and boundary conditions

Before addressing the problem of determination of the equations of motion and of the boundary conditions, one essential remark should be made. This is related to the fact that, in the context of the assumptions of symmetry and linearity of the structural model, the associated stretching and bending problems are decoupled. Thus, being interested in the eigenfrequencies related to the bending problem only, equations involving the stretching motion are discarded.

Hamilton's principle is used to derive the equations of motion and the boundary conditions of the bending theory of flat sandwich panels. It is formulated as

$$\delta J = \delta \int_{t_0}^{t_1} (U - W - T)\,\mathrm{d}t = 0, \tag{10}$$

where t_0, t_1 are two arbitrary instants of time, U denotes the strain energy, W denotes the work done by surface tractions, edge loads and body forces, T denotes the kinetic energy of the 3-D body of the sandwich structure, and δ is the variation operator. In Eq. (10)

$$\delta U = \frac{1}{2}\int_\sigma \left[\int_{\overline{h}}^{\overline{h}+h'} \sigma'_{ij}\delta e'_{ij} + \int_{-\overline{h}}^{+\overline{h}} \overline{\sigma}_{ij}\delta\overline{e}_{ij} + \int_{-\overline{h}-h''}^{-\overline{h}} \sigma''_{ij}\delta e''_{ij} \right] \mathrm{d}x_3\,\mathrm{d}\sigma, \quad (i,j = 1,2,3), \tag{11}$$

where σ_{ij} denotes the stress tensor and σ denotes the mid-plane area of the sandwich panel. In addition, as a result of Hamilton's condition, $\delta V_i = 0$ at t_0 and at t_1.

$$\int_{t_0}^{t_1} \delta T \, \mathrm{d}t = -\int_{t_0}^{t_1} \mathrm{d}t \left[\int_{\sigma} \int_{\overline{h}}^{\overline{h}+h'} \rho' \ddot{V}'_i \delta V'_i \, \mathrm{d}x_3 + \int_{-\overline{h}}^{\overline{h}} \overline{\rho} \ddot{\overline{V}}_i \delta \overline{V}_i \, \mathrm{d}x_3 + \int_{-\overline{h}-h''}^{-\overline{h}} \rho'' \ddot{V}''_i \delta V''_i \, \mathrm{d}x_3 \right], \tag{12}$$

$$\delta W = \int_{\sigma} \left[\int_{\overline{h}}^{\overline{h}+h'} \rho' H'_i \delta V'_i \, \mathrm{d}\sigma \, \mathrm{d}x_3 + \int_{-\overline{h}}^{\overline{h}} \overline{\rho} \overline{H}_i \delta \overline{V}_i \, \mathrm{d}\sigma \, \mathrm{d}x_3 + \int_{-\overline{h}-h''}^{-\overline{h}} \rho'' H''_i \delta V''_i \, \mathrm{d}\sigma \, \mathrm{d}x_3 \right] + \int_{\Omega_s} \underset{\sim}{\sigma}_i \delta V_i \, \mathrm{d}\Omega. \tag{13}$$

In Eq. (12) the superposed dots denote time derivatives, ρ denotes the mass density, $\underset{\sim}{\sigma}_i = \underset{\sim}{\sigma}_{ij} n_j$ denote the components of the stress vector prescribed on part Ω_σ of the external boundary Ω, n_i are the components of the outward unit vector normal to Ω, and H_i denote the components of the body force vector.

From Eq. (10) considered in conjunction with Eqs. (11)–(13), and with the strain–displacement relationships (used as subsidiary conditions), carrying out the integration with respect to x_3 and integrating by parts whenever feasible, using the expression of global stress resultants and stress couples (to be defined later), and invoking the arbitrary and independent character of variations $\delta\eta_1$, $\delta\eta_2$, δv_3 and $\delta v_{3,n}$ throughout the entire domain of the plate and within the time interval $[t_0, t_1]$, the equations of motion and the boundary conditions are derived. By retaining only transversal load and transversal inertia, the equations of motion associated with the bending problem are

$$\begin{aligned}
&\delta\eta_1 : L_{11,1} + L_{12,2} - \overline{N}_{13} = 0,\\
&\delta\eta_2 : L_{22,2} + L_{12,1} - \overline{N}_{23} = 0,\\
&\delta v_3 : -N^0_{11} v_{3,11} - N^0_{22} v_{3,22} + M_{11,11} + 2M_{12,12} + M_{22,22}\\
&\qquad + (1 + C_1/\overline{h})(\overline{N}_{13,1} + \overline{N}_{23,2}) + q_3(x_\alpha, t) - m_o \ddot{v}_3 = 0.
\end{aligned} \tag{14a–c}$$

In Eq. (14c), N^0_{11} and N^0_{22} are the normal edge loads considered to be positive in compression,

$$C_1 = (h' + h'')/4 \Longrightarrow h/2, \tag{15}$$

where the expression of C_1 corresponds to symmetric sandwich panels. In addition, $(\,)_{,\alpha}$ denotes partial differentiation with respect to surface coordinates x_α, while q_3 denotes the distributed transversal load that, within the context of the free vibration problem, should be discarded. Expressed in a condensed form, the associated boundary conditions on the edge $x_n = \text{constant}$ $(n = 1, 2)$ are

$$\begin{aligned}
&L_{nn} = \underset{\sim}{L}_{nn} && \text{or} \quad \eta_n = \underset{\sim}{\eta}_n,\\
&L_{nt} = \underset{\sim}{L}_{nt} && \text{or} \quad \eta_t = \underset{\sim}{\eta}_t,\\
&M_{nn} = \underset{\sim}{M}_{nn} && \text{or} \quad v_{3,n} = \underset{\sim}{v}_{3,n},\\
&M_{nn,n} + 2M_{nt,t} + (1 + C_1/\overline{h})\overline{N}_{n3} = \underset{\sim}{M}_{nt,t} + \underset{\sim}{\overline{N}}_{n3} && \text{or} \quad v_3 = \underset{\sim}{v}_3,
\end{aligned} \tag{16a–d}$$

where subscripts n and t are used to designate the normal and tangential in-plane directions to an edge, and hence $n = 1$ when $t = 2$, and vice versa. It should be noted that in this special case of pure bending, four boundary conditions have to be prescribed at each edge, implying that the equations governing the bending of flat sandwich panels should be of eighth order.

In Eqs. (14) and (16) the global stress resultants and stress couples are defined as

$$\begin{aligned}
&N_{11} = N'_{11} + N''_{11} \quad (1 \leftrightarrows 2)\\
&N_{12} = N'_{12} + N''_{12},\\
&L_{11} = \overline{h}(N'_{11} - N''_{11}) \quad (1 \leftrightarrows 2),\\
&L_{12} = \overline{h}(N'_{12} - N''_{12}),\\
&M_{11} = M'_{11} + M''_{11} \quad (1 \leftrightarrows 2)\\
&M_{12} = M'_{12} + M''_{12}.
\end{aligned} \tag{17a–f}$$

The sign $(1 \leftrightarrows 2)$ indicates that in Eqs. (17a,c,e) the expressions for stress resultants and stress couples not explicitly supplied can be obtained from the ones displayed above, by replacing subscripts 1 by 2 and vice versa. The same convention will be used throughout the paper. In Eqs. (17), the stress resultants and stress couples associated with the bottom face sheets are

$$\{N'_{\alpha\beta},\ M'_{\alpha\beta}\} = \sum_{k=1}^{N} \int_{(x_3)_{k-1}}^{(x_3)_k} (\sigma'_{\alpha\beta})_k \{1, x_3 - a'\}\, \mathrm{d}x_3 \quad (\alpha, \beta = 1, 2) \tag{18}$$

while the transverse shear stress measures in the core are defined as

$$\overline{N}_{\alpha 3} = \int_{-\overline{h}}^{\overline{h}} \overline{\sigma}_{\alpha 3}\, \mathrm{d}x_3. \tag{19}$$

The stress resultants and stress couples for the upper face can be obtained from Eqs. (16) by replacing single primes by double primes, a' by $-a''$, where, for the present case, $a' = a'' = a$. Herein, N is the number of constituent layers in the bottom face sheets, equal with that in the upper face sheets, while $(x_3)_k$ and $(x_3)_{k-1}$ denote the distances from the global reference plane (coinciding with that of the core layer) to the upper and bottom interfaces of the kth layer, respectively. Having in view that the top and bottom face sheets are symmetric with respect to both their mid-planes and with the mid-plane of the entire structure, considering that the materials of the face sheets exhibit monoclinic symmetry and that the core material is orthotropic, one can obtain the constitutive equations. These equations associated with the bottom face sheets reduced to the mid-plane of the structure are expressed in matrix form as

$$\begin{Bmatrix} N'_{11} \\ N'_{22} \\ N'_{12} \\ M'_{11} \\ M'_{22} \\ M'_{12} \end{Bmatrix} = \begin{bmatrix} A'_{11} & A'_{12} & A'_{16} & E'_{11} & E'_{12} & E'_{16} \\ A'_{21} & A'_{22} & A'_{26} & E'_{21} & E'_{22} & E'_{26} \\ A'_{16} & A'_{26} & A'_{66} & E'_{16} & E'_{26} & E'_{66} \\ E'_{11} & E'_{12} & E'_{16} & F'_{11} & F'_{12} & F'_{16} \\ E'_{21} & E'_{22} & E'_{26} & F'_{21} & F'_{22} & F'_{26} \\ E'_{16} & E'_{26} & E'_{66} & F'_{16} & F'_{26} & F'_{66} \end{bmatrix} \begin{Bmatrix} \varepsilon'_{11} \\ \varepsilon'_{22} \\ \gamma'_{12} \\ \kappa'_{11} \\ \kappa'_{22} \\ \kappa'_{12} \end{Bmatrix}. \tag{20}$$

The stiffness quantities appearing in Eq. (19) are defined as

$$\{A'_{\omega\rho},\ D'_{\omega\rho}\} = \{A''_{\omega\rho},\ D''_{\omega\rho}\} = \sum_{k=1}^{n'} \int_{(x_3)_{k-1}}^{(x_3)k} (\hat{Q}'_{\omega\rho})_{(k)} (1, x_3^2)\, \mathrm{d}x_3 \quad (\omega, \rho = 1, 2, 6). \tag{21}$$

$\hat{Q}_{\omega\rho}$ is the reduced elastic moduli, where for a symmetric construction, $\hat{Q}'_{\omega\rho} = \hat{Q}''_{\omega\rho}$, while

$$E'_{\omega\rho} = a' A'_{\omega\rho} = -E''_{\omega\rho}; \quad F'_{\omega\rho} = D'_{\omega\rho} + a'^2 A'_{\omega\rho} = F''_{\omega\rho} \equiv F_{\omega\rho}. \tag{22a,b}$$

The expression of stress resultants and stress couples for the upper facing can be obtained from their counterparts associated with the bottom face sheets by replacing the single prime by double primes. For the weak core layer considered as an orthotropic body (the axes of orthotropy coinciding with the geometrical axes), the constitutive equations are

$$\bar{N}_{13} = 2\bar{h}\bar{K}^2 \bar{Q}_{55} \bar{\gamma}_{13}, \quad \bar{N}_{23} = 2\bar{h}\bar{K}^2 \bar{Q}_{44} \bar{\gamma}_{23}, \tag{23a,b}$$

where $\bar{K}^2$ is the shear transverse correction factor, while $\overline{Q}_{55}$ $(\equiv \overline{Q}_{13})$ and $\overline{Q}_{44}$ $(\equiv \overline{G}_{23})$ are the transverse shear moduli.

5. Governing equations for flexural motion

The equations of flexural motion of sandwich plates expressed in terms of displacement quantities η_1, η_2 and v_3 are given by [12]:

$$\begin{aligned}
\delta\eta_1 : & A_{11}\eta_{1,11} + A_{66}\{\eta_{1,22} + \eta_{2,12}\} + A_{12}\eta_{2,12} + A_{16}\{2\eta_{1,12} + \eta_{2,11}\} \\
& + A_{26}\eta_{2,22} - d_1\{\eta_1 + av_{3,1}\} = 0, \\
\delta\eta_2 : & A_{22}\eta_{2,22} + A_{66}\{\eta_{2,11} + \eta_{1,12}\} + A_{12}\eta_{1,12} + A_{26}\{2\eta_{2,12} + \eta_{1,22}\} \\
& + A_{16}\eta_{1,11} - d_2\{\eta_2 + av_{3,2}\} = 0, \\
\delta v_3 : & -F_{11}v_{3,1111} - F_{22}v_{3,2222} - 2F_{12}v_{3,1122} - 4F_{16}v_{3,1112} - 4F_{26}v_{3,1222} \\
& - 4F_{66}v_{3,1122} + d_1a\{\eta_{1,1} + av_{3,11}\} + d_2a\{\eta_{2,2} + av_{3,22}\} \\
& - N_{11}^0 v_{3,11} - N_{22}^0 v_{3,22} - m_0\ddot{v}_3 = 0.
\end{aligned} \tag{24a–c}$$

In Eqs. (24)

$$\{d_1, d_2\} = (2\overline{K}^2/\overline{h})\{\overline{G}_{13}, \overline{G}_{23}\}, \tag{24d}$$

while m_0 is the reduced mass per unit mid-plane area:

$$m_0 = \int_{-\overline{h}}^{-\overline{h}-h''} \rho_{(k)}'' \,\mathrm{d}x_3 + \int_{-\overline{h}}^{\overline{h}} \overline{\rho}\,\mathrm{d}x_3 + \int_{\overline{h}}^{\overline{h}+h'} \rho_{(k)}' \,\mathrm{d}x_3, \tag{24e}$$

ρ being the mass-density of the constituent material. As is clear from Eq. (22a), due to the symmetry with respect to the structural mid-plane, the stiffness quantities $E_{\omega\rho}$ exactly vanish.

6. Solution methodology

The problem of determination of eigenfrequencies of sandwich panels reduces to the solution of an eigenvalue problem. Due to the intricacy of the governing equations and the boundary conditions, an approximate solution methodology will be applied. The method will be illustrated for the case of rectangular sandwich panels simply supported on $x_1 = 0, L_1$, and $x_2 = 0, L_2$. For the bending problem, the boundary conditions along the edges $x_n = 0$, L_n, are

$$\eta_n = 0, \quad \eta_t = 0, \quad M_{nn} = 0, \quad v_3 = 0. \tag{25a–d}$$

The strategy is to identically fulfil Eqs. (24a,b), and fulfil Eq. (24c) and the boundary conditions (25a,b) in the Galerkin sense. To this end, we use, for the displacement quantities, the representations

$$v_3(x_1, x_2, t) = W_{mn} \sin\lambda_m x_1 \sin\mu_n x_2 \exp(\mathrm{i}\omega_{mn} t), \tag{26a}$$

$$\eta_1(x_1, x_2, t) = [H_1^{(m,n)} \cos\lambda_m x_1 \sin\mu_u x_2 + H_2^{(m,n)} \sin\lambda_m x_1 \cos\mu_n x_2] \exp(\mathrm{i}\omega_{mn} t), \tag{26b}$$

$$\eta_2(x_1, x_2, t) = [I_1^{(m,n)} \cos\lambda_m x_1 \sin\mu_n x_2 + I_2^{(m,n)} \sin\lambda_m x_1 \cos\mu_n x_2] \exp(\mathrm{i}\omega_{mn} t), \quad \sum\!\!\!\!\!\!\diagup_{m,n}. \tag{26c}$$

In these equations W_{mn}, $H^{(m,n)}$ and $I^{(m,n)}$ are arbitrary coefficients; $\mathrm{i} = \sqrt{-1}$, $\lambda_m = m\pi/L_1$, $\mu_n = n\pi/L_2$; L_1 and L_2 are the panel length and width, respectively, ω_{mn} are the natural frequencies, while the sign $\sum\!\!\!\!\!\!\diagup_{m,n}$ indicates that in Eqs. (26) there is no summation over indices m and n.

Substituting representations (26) in Eqs. (24a,b) and identifying the coefficients of the same trigonometric functions results in a system of equations expressed in matrix form as

$$\begin{bmatrix} U_{11}^{(m,n)} & U_{12}^{(m,n)} & U_{13}^{(m,n)} & U_{14}^{(m,n)} \\ U_{12}^{(m,n)} & U_{11}^{(m,n)} & U_{14}^{(m,n)} & U_{13}^{(m,n)} \\ U_{13}^{(m,n)} & U_{14}^{(m,n)} & U_{33}^{(m,n)} & U_{34}^{(m,n)} \\ U_{14}^{(m,n)} & U_{13}^{(m,n)} & U_{34}^{(m,n)} & U_{33}^{(m,n)} \end{bmatrix} \begin{Bmatrix} H_1^{(m,n)} \\ H_2^{(m,n)} \\ I_1^{(m,n)} \\ I_2^{(m,n)} \end{Bmatrix} = \begin{Bmatrix} V_1^{(m,n)} \\ 0 \\ 0 \\ V_2^{(m,n)} \end{Bmatrix}. \tag{27}$$

The elements $U_{ij}^{(m,n)}$ of the matrix are functions of the geometrical and mechanical characteristics of the sandwich panel. Their expressions are not supplied here, while

$$V_1^{(m,n)} = -d_1 am(L_1/\pi)W_{mn}, \quad V_2^{(m,n)} = -d_2 an\phi(L_1/\pi)W_{mn}. \tag{28a,b}$$

From Eq. (27) one obtains the expressions of $H^{(m,n)}$ and $I^{(m,n)}$ that are non-zero, namely

$$H_1^{(m,n)} = \tilde{H}_1^{(m,n)} W_{mn}, \quad I_2^{(m,n)} = \tilde{I}_2^{(m,n)} W_{mn}, \quad \sum_{m,n}, \tag{29a,b}$$

where

$$\tilde{H}_1^{(m,n)} = \frac{a\{[(A_{12}+A_{66})d_2 - A_{22}d_1]\lambda_m\mu_n^2 - d_1A_{66}\lambda_m^3 - d_1d_2\lambda_m\}}{\Delta_{mn}},$$

$$\tilde{I}_2^{(m,n)} = \frac{a\{[(A_{12}+A_{66})d_1 - A_{11}d_2]\lambda_m^2\mu_n - d_2A_{66}\mu_n^3 - d_1d_2\mu_n\}}{\Delta_{mn}} \tag{30a,b}$$

while

$$\begin{aligned}\Delta_{mn} = {} & A_{11}A_{66}\lambda_m^4 + (d_2A_{11} + d_1A_{66})\lambda_m^2 + (A_{11}A_{22} - 2A_{12}A_{66} - A_{12}^2)\lambda_m^2\mu_n^2 \\ & + (d_1A_{22} + d_2A_{66})\mu_n^2 + A_{22}A_{66}\mu_n^4 + d_1d_2.\end{aligned} \tag{30c}$$

It should be remarked that Eq. (30b) can be obtained from Eq. (30a) by replacing d_2 with d_1 and vice versa, and replacing λ_m with μ_n and vice versa, while Eq. (30c) remains invariant under these transformations. Substituting displacement representations (26) into Eq. (10) (Hamilton's principle), performing the required integrations, and keeping in mind that Eqs. (24a,b) and the geometrical boundary conditions (25c,d) are identically satisfied results in an eigenvalue problem that yields the following closed-form expression of dimensionless eigenfrequencies:

$$\begin{aligned}\Omega_{mn}^2 = {} & m^4 + \frac{F_{22}n^4\phi^4}{F_{11}} + \frac{2(F_{12}+2F_{66})m^2n^2\phi^2}{F_{11}} + \frac{a^2L_1^2}{F_{11}\pi^2}(d_1m^2 + d_2n^2\phi^2) \\ & + \frac{aL_1^3}{F_{11}\pi^3}(d_1m\tilde{H}_1^{(m,n)} + d_2n\phi\tilde{I}_2^{(m,n)}) - K_x(m^2\pi^2 + L_Rn^2\pi^2\phi^{2\phi}).\end{aligned} \tag{31}$$

Herein, the dimensionless eigenfrequencies, the normalized edge loads and the panel aspect ratio are defined as

$$\Omega_{mn}^2 \equiv \frac{m_0L_1^4}{\pi^4F_{11}}\omega_{mn}^2, \quad K_x \equiv \frac{L_1^2N_{11}^0}{\pi^4F_{11}}, \quad K_y \equiv \frac{L_1^2N_{22}^0}{\pi^4F_{11}}, \quad L_R \equiv N_{22}^0/N_{11}^0, \quad \phi \equiv L_1/L_2. \tag{32a–e}$$

In spite of the evident complexity of the problem, the closed-form solution of eigenfrequencies of sandwich panels with laminated anisotropic face sheets as expressed by Eq. (31) constitutes a remarkable result.

7. Numerical simulations

Before carrying out a numerical analysis enabling one to highlight the influence played by a number of essential parameters proper to anisotropic sandwich structures, a validation of the analytical predictions obtained as per the present structural model against those available in the literature is in order. To this end,

Table 1
Material and geometric characteristics

	Thickness in. (mm)	Elastic Modulus lb/in.^{2} (GPa)	Poisson's ratio	Mass density lb s^2/in.^{4} (N s^2 m^{-4})	Shear Modulus lb/in.^{2} (GPa)
Upper face	0.016 (0.4064)	10^7 (68.95)	0.33	2.59×10^{-4} (2768.93)	3.76×10^6 (25.92) (G_{12})
Lower face	0.016 (0.4064)	10^7 (68.95)	0.33	2.59×10^{-4} (2768.93)	3.76×10^6 (25.92) (G_{12})
Core	0.250 (6.35)	0	0	1.14×10^{-5} (121.83)	7500 (0.0517) 19500 (0.134) ($\overline{G}_{13}$) ($\overline{G}_{23}$)

Table 2
Eigenfrequency predictions

ω_{ij} (Hz)	Experiment [14]	Exact [14]	FEM [15]	SFPM [16]	Present
ω_1 ($=\omega_{11}$)	–	23	23	23.30	23.40
ω_2 ($=\omega_{21}$)	45	44	44	44.48	44.64
ω_3 ($=\omega_{12}$)	69	71	70	71.36	71.51
ω_4 ($=\omega_{31}$)	78	80	80	78.81	79.27
ω_5 ($=\omega_{22}$)	92	91	90	91.90	92.2
ω_6 ($=\omega_{32}$)	125	126	125	125.16	125.97

Table 3
Critical Buckling Load

Layup $[\theta/-\theta/\theta/\text{Core}/\theta/-\theta/\theta]$						
θ (deg)	ψ ($\equiv L_1/L_2$)	L_1 in. (m)	F_{11} lb in. (N/m)	K_{cr}	(N^0_{11})cr , lb/in. (N/m) [1]	(N^0_{11})cr, lb/in. (N/m) [Present]
47	1.11	24 (0.6096)	9.8685 (1728.2)	7110.28	11 865 (2.08×10^6)	11 866.34 (2.08×10^6)
44.1	1.00	24 (0.6096)	11.5027 (2014.5)	4913.96	9559 (1.67×10^6)	9558.94 (1.67×10^6)
38.6	0.833	24 (0.6096)	15.0207 (2630.6)	2734.11	6945.5 (1.22×10^6)	6945.17 (1.22×10^6)
31.5	0.714	24 (0.6096)	20.0690 (3514.7)	1664.60	5649 (0.99×10^6)	5649.53 (0.99×10^6)
19.8	0.625	24 (0.6096)	28.2660 (4950.2)	1056.09	5048.3 (0.88×10^6)	5048.27 (0.88×10^6)

the case of a three-layer rectangular sandwich panel ($L_1 = 72$ in. (1.828 m), $L_2 = 48$ in. (1.219 m)) whose faces are of aluminum and a core of aluminum honeycomb is considered. Their geometric and elastic characteristics are displayed in Table 1.

The various mode eigenfrequencies obtained in Ref. [14] via experiments and via an exact approach, in Ref. [15] via FEM, and in Ref. [16] via the spline finite point method (SFPM) are compared with those derived via the present closed-form solution, Eq. (31). The results are summarized in Table 2. The supplied results reveal an excellent agreement of the actual predictions with those obtained by various methods.

Another validation concerns the buckling load of anisotropic sandwich panels obtained at such values of the compressive edge load for which the eigenfrequencies vanish. In this connection, in Fig. 2, for the case of a sandwich plate featuring the stacking sequence $[\theta/-\theta/\theta/\text{core}/\theta/-\theta/\theta]$, the buckling loads are obtained for selected panel aspect ratios ϕ from the variation of the fundamental dimensionless eigenfrequency $\Omega_{11}^{1/2}$ vs. K_x. Table 3 shows critical buckling loads $(K_x)_{cr}$ obtained from Eq. (31) at such values of K_x for which $\Omega_{11}^{1/2}$ vanishes, as well as those obtained in Ref. [12], via a direct buckling approach. At this point one should recall the fact (see e.g. Ref. [13]) that in conditions in which a compressive edge load exists, the requirement of zero eigenfrequency results in static instability, generally referred to as the *divergence* corresponding, in this case, to buckling. On the other hand, in Ref. [12], buckling was addressed as a problem per se, i.e. as the solution of an eigenvalue problem. Also these results reveal an excellent agreement with predictions.

Table 4
Material properties for the face sheets

Type	Material	E_1, Msi (GPa)	E_2, Msi (GPa)	G_{12}, Msi (GPa)	ν_{12}
$F1$	HS graphite epoxy	26.25 (180.99)	1.5 (10.34)	1.05 (7.24)	0.28
$F2$	IM7/977-2	11.6 (79.98)	10.9 (75.15)	1.4 (9.65)	0.06

Table 5
Material properties for the core

Type	Core type, honeycomb	$\bar{G}_{13}$, Msi (GPa)	$\bar{G}_{23}$, Msi (GPa)
$C1$	Titanium	0.20835 (1.44)	0.09435 (0.651)

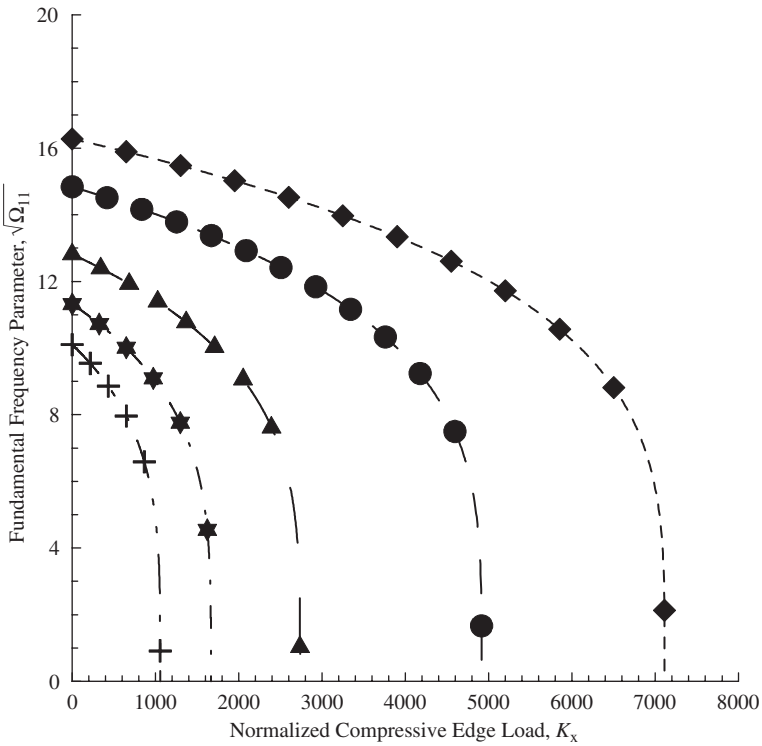

Fig. 2. Variation of dimensionless eigenfrequency $\Omega_{11}^{1/2}$ vs. K_x for selected θ and ϕ^1 ($\equiv L_1/L_2$). The panel lay-up is $[\theta/-\theta/\theta/\text{core}/\theta/-\theta/\theta]$, $\hat{h} = 0.02$ in. (0.508 mm). [- - -, $\theta = 47^\circ$; ——, $\theta = 44.1^\circ$; ——, $\theta = 38.6^\circ$; ——·——, $\theta = 31.5^\circ$; ——··——, $\theta = 19.8^\circ$]. (◆) $\phi = 1.11$; (●) $\phi = 1.0$; (▲) $\phi = 0.833$; (★) $\phi = 0.714$; (+) $\phi = 0.625$.

In these latter results as well as in forthcoming ones, material properties for the face sheets and the core are listed in Tables 4 and 5. In addition, in all simulations included in Figs. 2–13, $L_1 = 24$ in. (0.6096 m), $\overline{h} = 0.5$ in. (0.0127 m), and unless otherwise specified, the faces and the core are considered to be made up from $F1$ and $C1$ materials, respectively. Their properties are supplied in Tables 4 and 5.

Moreover, with the exception of cases in Figs. 2, 12 and 13, where $\hat{h} = 0.02$ in. (0.508×10^{-3} m) in the remaining figures, $\hat{h} = 0.005$ in. (0.0127×10^{-2} m) was considered.

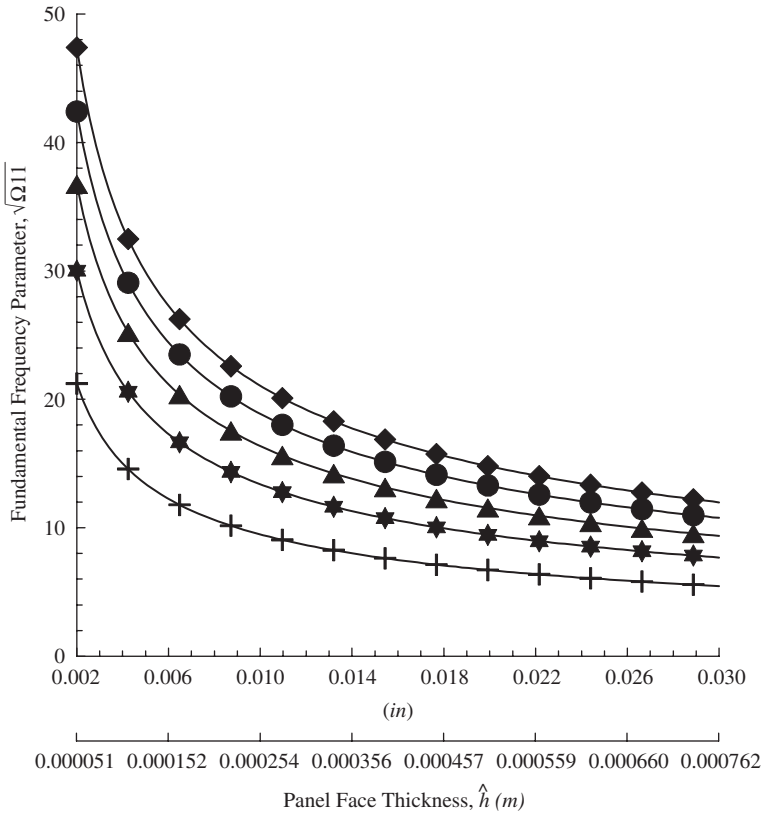

Fig. 3. Variation of the dimensionless fundamental eigenfrequency $\Omega^{1/2}$ vs. total face sheet thickness $\hat{h}$ for selected values of a; $\phi = 1$. The panel lay-up is [45°/core/45°]. (◆) $a = 0.5$ in. (0.0127 m); (●) $a = 0.4$ in. (0.0128 m); (▲) $a = 0.3$ in. (0.00762 m); (★) $a = 0.2$ in. (0.00508 m); (+) $a = 0.1$ in. (0.00254 m).

Following the validation of both the structural model and the solution methodology, numerical simulations highlighting the implications of various effects on eigenfrequencies will be displayed. The effects of panel face thickness considered in conjunction with that of distance a on the dimensionless fundamental eigenfrequency, $\Omega_{11}^{1/2}$ are displayed in Fig. 3. From this figure the strong influence of face thickness $\hat{h}$ and distance a on the fundamental dimensionless eigenfrequency $\Omega_{11}^{1/2}$ can be considered. In the expression of $\Omega_{11}^{1/2}$, the normalizing quantity F_{11} that depends on both h^3 and a^2h is involved; thus the variation of $\Omega_{11}^{1/2}$ as a function of $\hat{h}$ and a reveals an opposite trend to that normally featured by its dimensional counterpart as a function of the same geometrical parameters. In this sense, the results reveal a decay of $\Omega_{11}^{1/2}$ as a function of the increase of $\hat{h}$, and a decrease that is more severe as a increases.

The effect of the directional property of the material of face sheets on dimensionless eigenfrequency $\Omega_{11}^{1/2}$ is addressed in various contexts in Figs. 4–12. Fig. 4 displays the effect of the ply-angle of face sheets considered in conjunction with that of the panel aspect ratio ϕ on dimensionless fundamental eigenfrequency $\Omega_{11}^{1/2}$. In this case, the stacking sequence of the sandwich panel is $[\theta/\text{core}/\theta]$. The face sheets and the core are made up from materials $F1$ and $C1$, respectively.

It clearly appears that with the decrease of L_2, i.e. with the increase of ϕ, the increase of the ply-angle until $\theta = \pi/2$ is accompanied by the increase of $\Omega_{11}^{1/2}$. In contrast to this trend, for the case face sheets made up of material $F2$ that features a very low orthotropicity ratio, the behavior shown in Fig. 4 is replaced by that shown in Fig. 5, where in addition to the rather reduced sensitivity of the variation of $\Omega_{11}^{1/2}$ with that of θ, a shift of their maxima towards $\theta = \pi/4$ ply-angles is revealed. For the same stacking sequence as before, the implications of the ply-angle of face sheets on various mode eigenfrequencies are given in Figs. 6 and 7. It

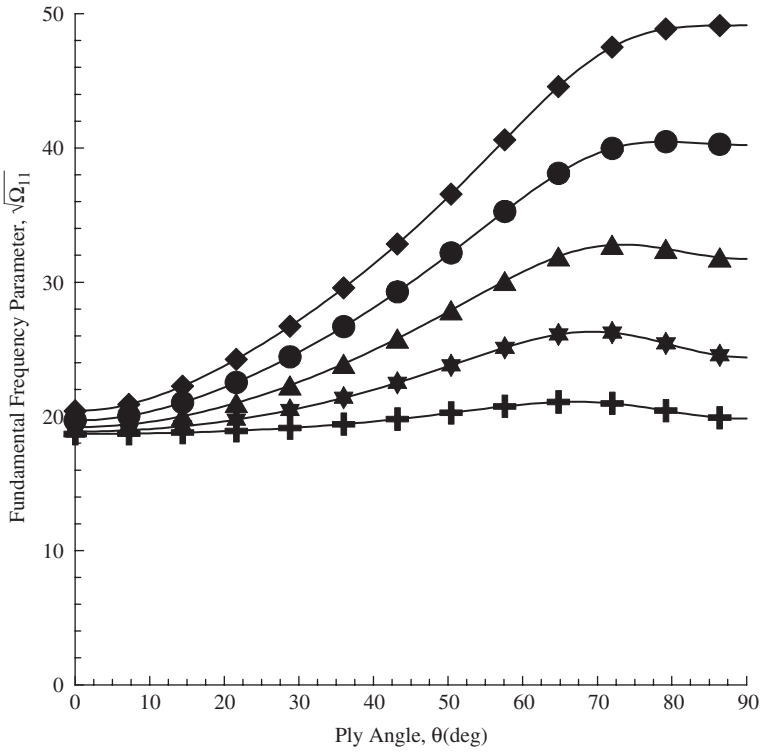

Fig. 4. Variation of the dimensionless fundamental eigenfrequency $\Omega_{11}^{1/2}$ vs. ply-angle for selected values of the parameter ϕ. Faces and core are from $F1$ and $C1$, respectively; the panel lay-up is $[\theta/\text{core}/\theta]$. (◆) $\phi = 1.25$; (●) $\phi = 1.0$; (▲) $\phi = 0.75$; (★) $\phi = 50$; (+) $\phi = 0.25$.

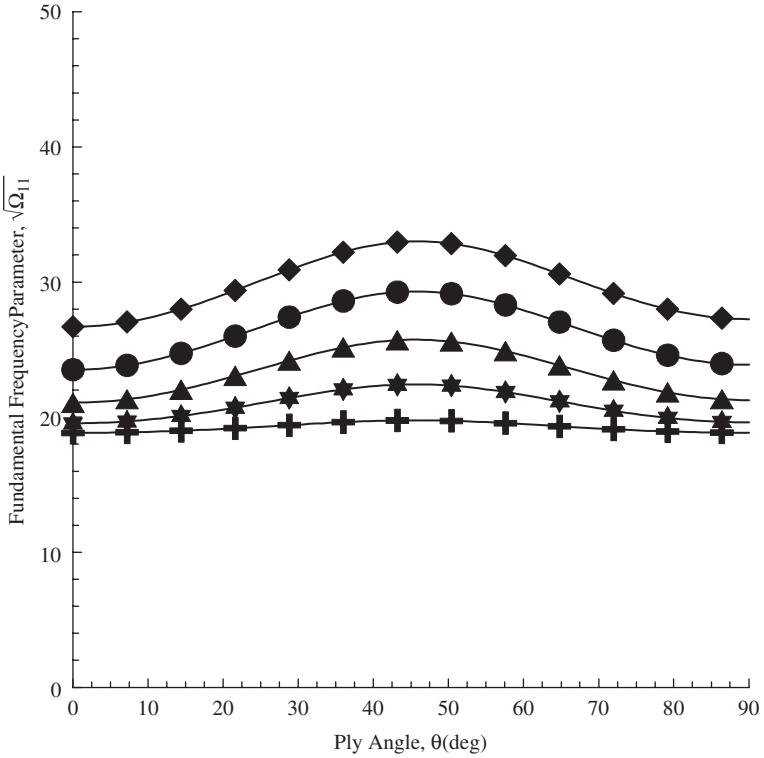

Fig. 5. Counterpart of Fig. 4 for the case of face sheets made up of $F2$. The panel lay-up is $[\theta/\text{core}/\theta]$. (◆) $\phi = 1.25$; (●) $\phi = 1.0$; (▲) $\phi = 0.75$; (★) $\phi = 0.5$; (+) $\phi = 0.25$.

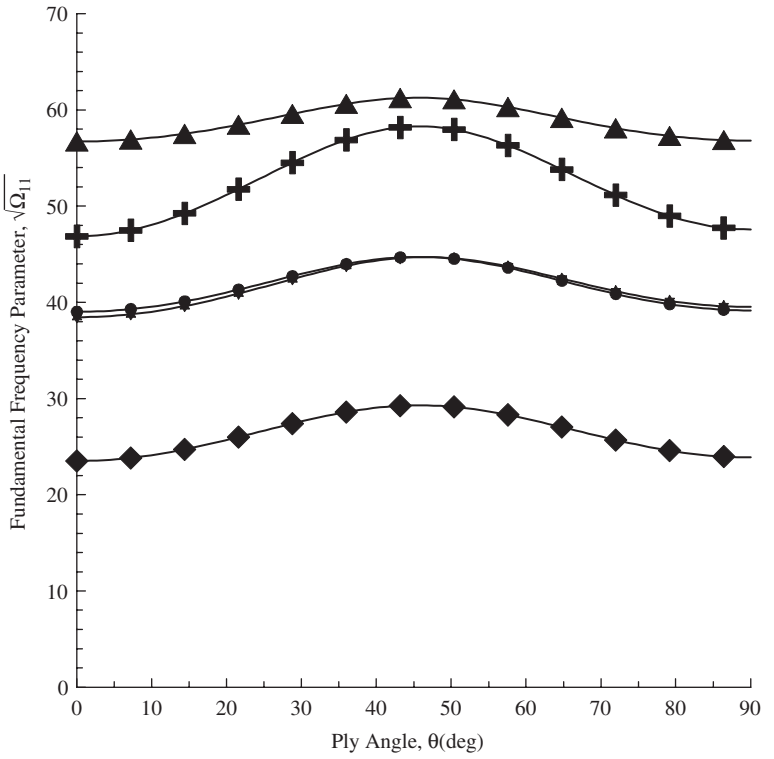

Fig. 6. Effects of the ply-angle on various dimensionless mode eigenfrequencies $\Omega_{mn}^{1/2}$. The panel lay-up is $[\theta/\text{core}/\theta]$, the face sheets and the core being made up of $F1$ and of $C1$ materials, respectively. (+) $m=1, n=1$; (⋆) $m=2, n=1$; (▲) $m=3, n=1$; (•) $m=1, n=2$; (◆) $m=2, n=2$.

clearly appears that in the case of face sheet materials $F1$ and $F2$, the trend of variation of dimensionless eigenfrequencies vs. θ follows those highlighted for $\Omega_{11}^{1/2}$ in Figs. 4 and 5, respectively.

Fig. 8 presents the effect of orthotropicity ratio λ $(=E_1/E_2)$ coupled with that of ply-angle on the variation of the dimensionless fundamental eigenfrequency $\Omega_{11}^{1/2}$. In this case the stacking sequence of the structure is $[\theta/\text{core}/\theta]$. The results shown in this plot reveal that an increase in the orthotropicity ratio, implying in this case an increase in E_1, plays a beneficial role in the increase of $\Omega_{11}^{1/2}$, especially for values of $\theta > 45^\circ$. Figs. 9a,b correspond to the panel lay-ups $[45^\circ/\text{core}/45^\circ]$ and $[30^\circ/\text{core}/30^\circ]$, respectively, where the coupling effects of both panel aspect ratio and orthotropicity ratio λ are highlighted. The results in both plots reveal that the panel aspect ratio has a strong effect on the variation of $\Omega_{11}^{1/2}$. At the same time, these figures reveal that, depending on the panel lay-up, the effect of the increase of the orthotropicity ratio can be beneficial, in the sense of an increase in $\Omega_{11}^{1/2}$ (see Fig. 9a), or detrimental (see Fig. 9b), in the sense of a decrease in $\Omega_{11}^{1/2}$. This difference in trend is consistent with the results emerging from Fig. 8. However, as might be observed from the results shown in Fig. 8 for another stacking sequence such as $[60^\circ/\text{core}/60^\circ]$, the increase of λ coupled with that of ϕ can result in larger increases of $\Omega_{11}^{1/2}$ than those shown in Fig. 9a, while for the stacking sequence $[0^\circ/\text{core}/0^\circ]$, an exacerbation of the trend featured in Fig. 9b is expected to occur.

Figs. 10 and 11 show the implications of varying the core transverse shear ratio η $(\equiv \overline{G}_{13}/\overline{G}_{23})$ on the first dimensionless eigenfrequency $\Omega_{11}^{1/2}$. It is assumed that $\overline{G}_{13}$ is fixed $(=1.44\,\text{GPa})$ and therefore, only $\overline{G}_{23}$ varies. While in Fig. 11 the implications on $\Omega_{11}^{1/2}$ of the variation of both η and θ are highlighted, in Fig. 10 those of η and ϕ are put into evidence. From these plots it becomes evident that for $\phi > 2$, the effect of η becomes increasingly accentuated. In this sense, it is seen that with its decrease, implying for this case an increase of $\overline{G}_{23}$, an increase of $\Omega_{11}^{1/2}$ results. The coupling effect of the increase of θ with the decrease of η, that is with the increase of $\overline{G}_{23}$, also provides a strong increase of $\Omega_{11}^{1/2}$.

Finally, Figs. 12 and 13 highlight the effects of the normalized compressive edge load coupled with that of the ply-angle θ, and of the biaxial compressive edge load-ratio L_R $(\equiv K_y/K_x)$ in conjunction with that of K_x

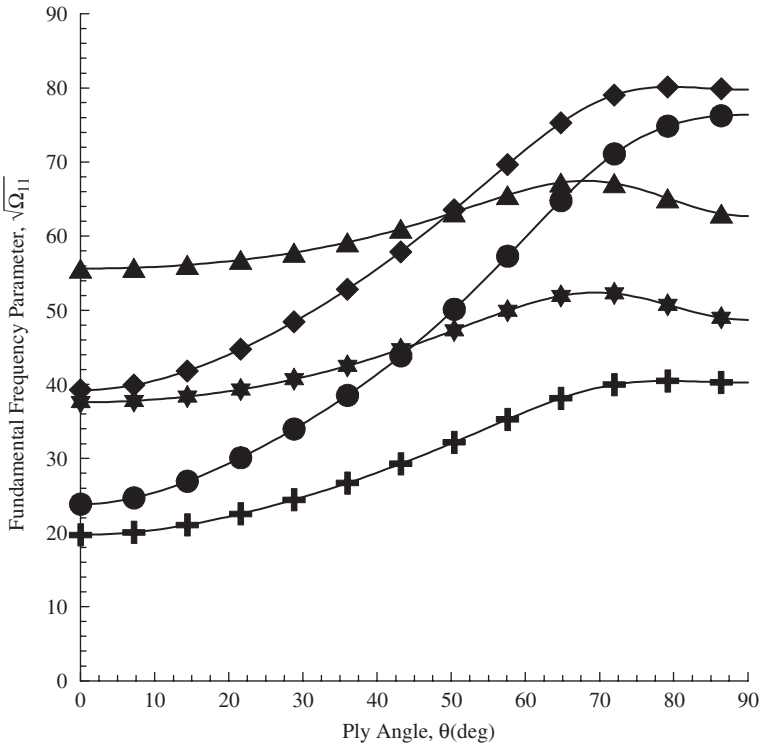

Fig. 7. Counterpart of Fig. 6 for the case of face sheets made up of $F2$. The panel lay-up is $[\theta/\text{core}/\theta]$. (◆) $m=1,n=1$; (●) $m=2,n=1$; (▲) $m=3,n=1$; (★) $m=1,n=2$; (+) $m=2,n=2$.

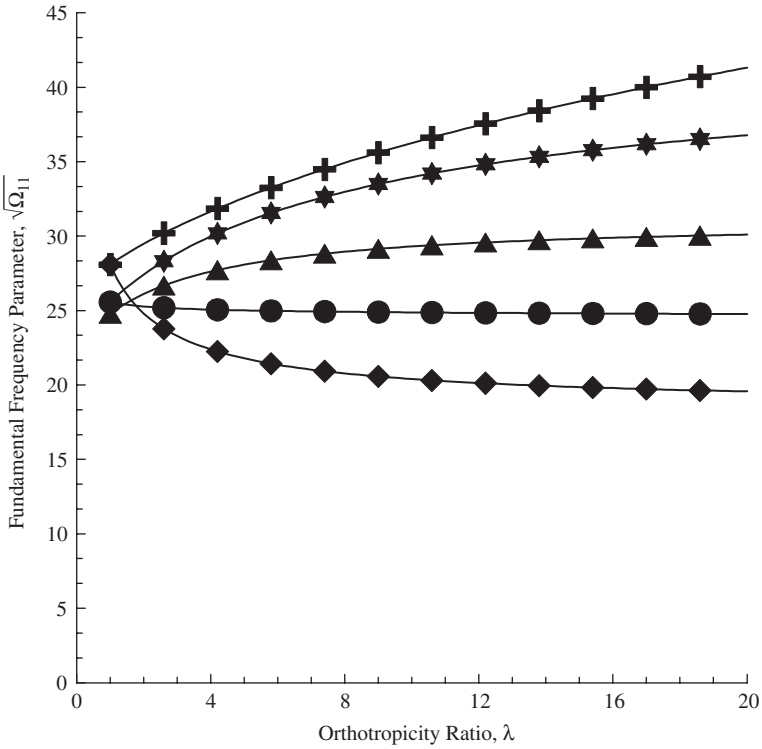

Fig. 8. Implications of orthotropicity ratio $\lambda\,(=E_1/E_2)$ coupled with that of θ on $\Omega_{11}^{1/2}$; $\phi=1$; $E_2=10.34\,\text{GPa}$; $G_{12}=7.24\,\text{GPa}$; $\nu_{12}=0.28$, lay-up $[\theta/\text{core}/\theta]$. (◆) $\theta=0^\circ$; (●) $\theta=30^\circ$; (▲) $\theta=45^\circ$; (★) $\theta=60^\circ$; (+) $\theta=90^\circ$.

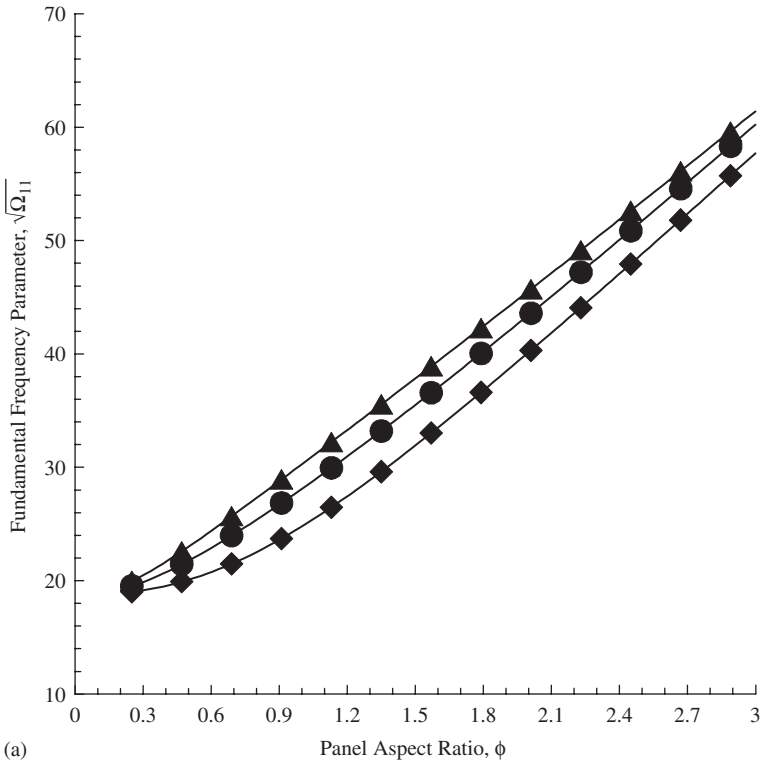

(a)

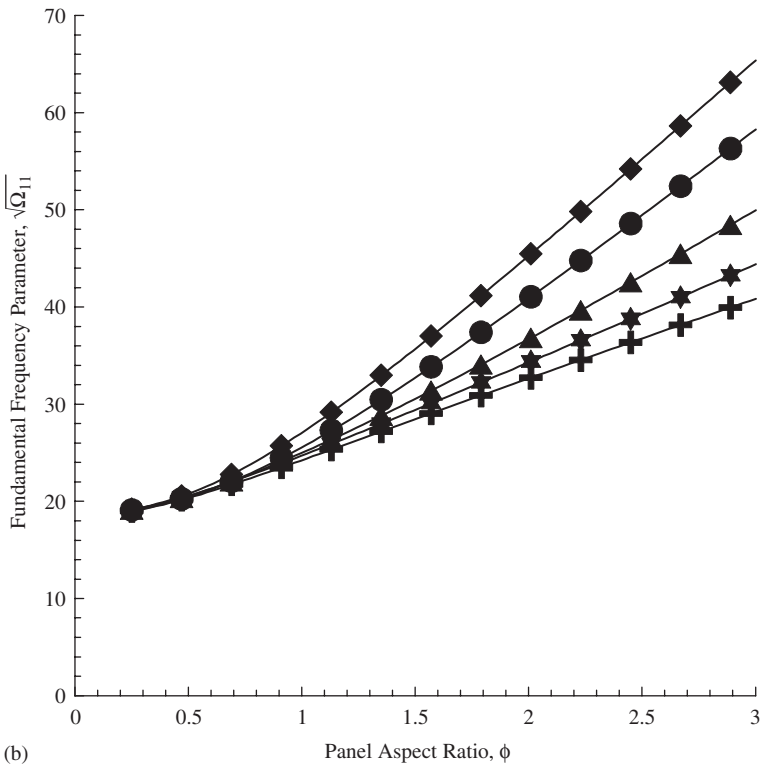

(b)

Fig. 9. Implications of panel aspect ratio coupled with that of orthotropicity ratio λ ($\equiv E_1/E_2$) on $\Omega_{11}^{1/2}$. The material characteristics of face sheets are as in Fig. 8. (a) The panel lay-up is [45°/core/45°]; (◆) $\lambda = 1$; (●) $\lambda = 5$; (▲) $\lambda = 25$; (b) The panel lay-up is [30°/core/30°] (◆) $\lambda = 0.2$; (●) $\lambda = 1$; (▲) $\lambda = 25$; (⋆) $\lambda = 25$; (+) $\lambda = 125$.

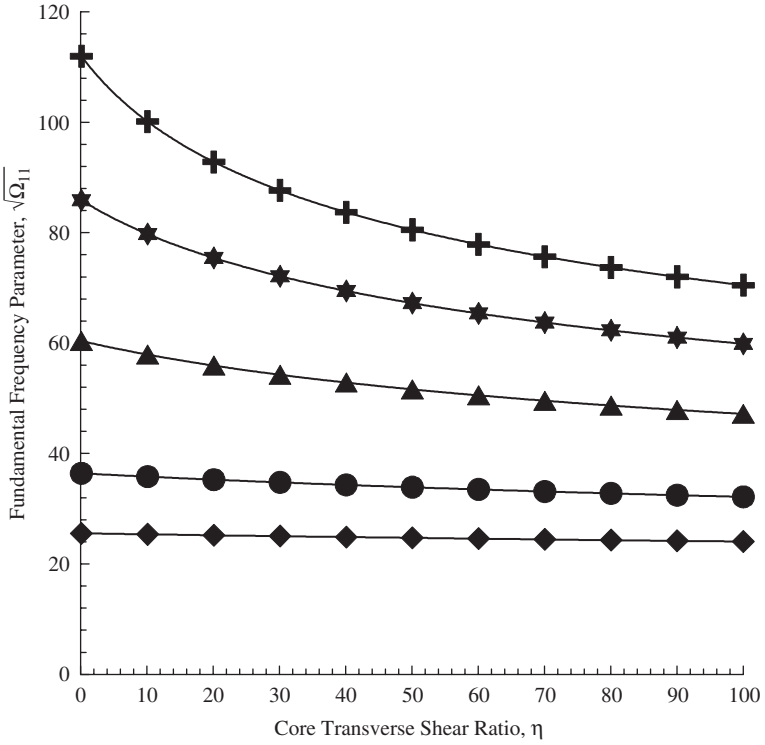

Fig. 10. Implications of transverse shear orthotropy ratio of the core, η, coupled with that of ϕ on $\Omega_{11}^{1/2}$, lay-up [60°/core/60°], $\overline{G}_{13} = 1.44\,\text{GPa}$. (◆) $\phi = 0.5$; (●) $\phi = 1.0$; (▲) $\phi = 2.0$; (★) $\phi = 3.0$; (+) $\phi = 4.0$.

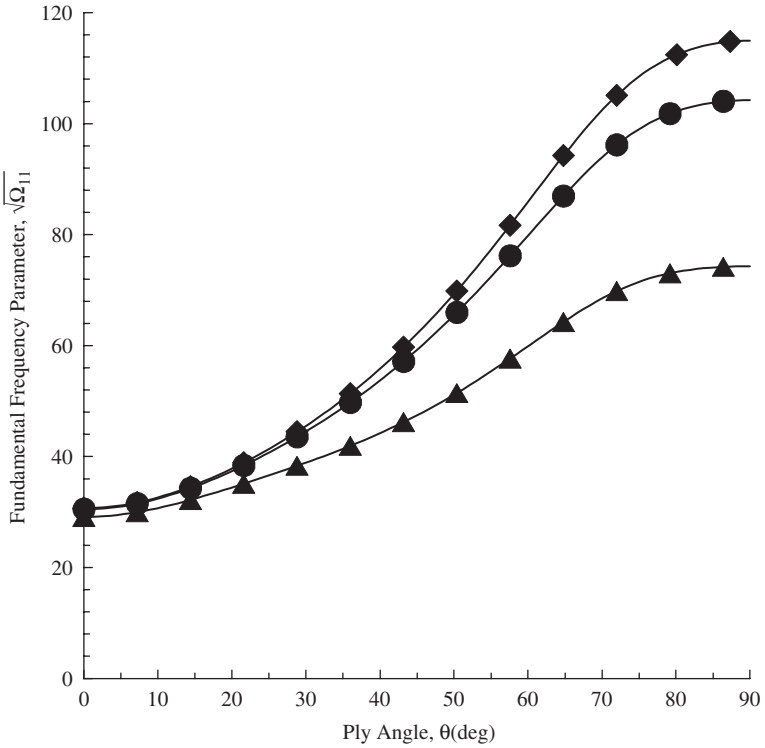

Fig. 11. Implications of transverse shear orthotropy ratio of the core η ($\equiv \overline{G}_{13}/\overline{G}_{23}$), and ply-angle of faces, on the dimensionless fundamental eigenfrequency; $\overline{G}_{13} = 1.44\,\text{GPa}$, $\phi = 3$, lay-up [θ/core/θ]. (◆) $\eta = 0.1$; (●) $\eta = 10$; (▲) $\eta = 100$.

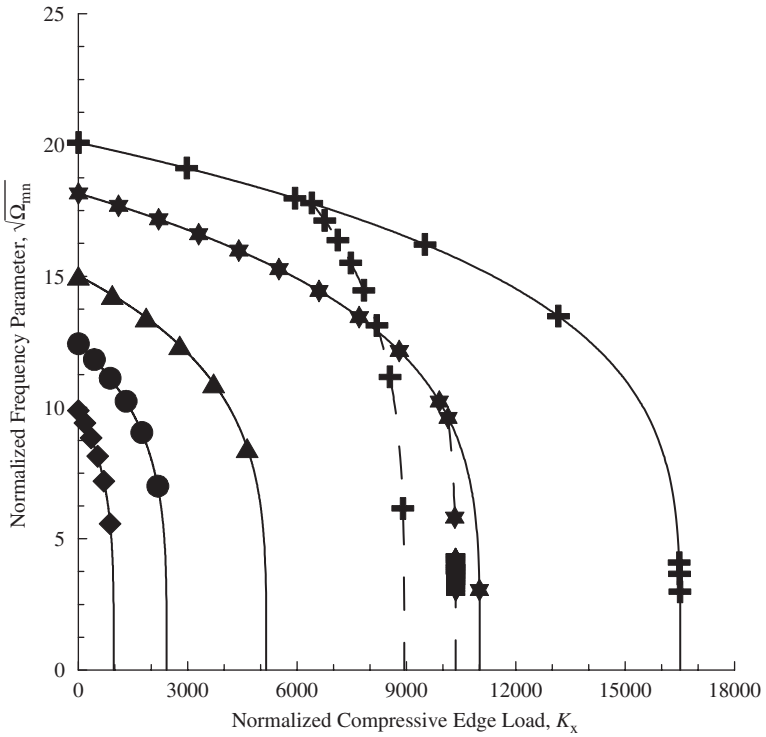

Fig. 12. Implications of uniaxial compressive edge load and of face sheet ply-angle on the dimensionless eigenfrequency $\Omega_{11}^{1/2}$ of the sandwich panel, $\hat{h} = 0.02$ in. (0.508 mm), $\phi = 1$. The panel lay-up is $[\theta/-\theta/\theta/\text{core}/\theta/-\theta/\theta]$. For $\theta = 60^\circ$ and 90° in order to capture the corresponding minimum buckling loads, the variations of $\Omega_{21}^{1/2}$ vs. K_x have been also included (—, $m = 1$, $n = 1$; - - -, $m = 2$, $n = 1$). (◆) $\theta = 0^\circ$; (●) $\theta = 30^\circ$; (▲) $\theta = 45^\circ$; (★) $\theta = 60^\circ$; (+) $\theta = 90^\circ$.

on dimensionless $(\Omega_{mn})^{1/2}$, respectively. It should be noted that $L_R > 0$, $L_R = 0$ and $L_R < 0$ correspond to $K_y > 0$ (compression), $K_y = 0$, or $K_y < 0$ (tension), respectively. The results of Fig. 12 reveal that the ply-angle θ of face sheets plays an enormously beneficial role in the increase of both the eigenfrequencies and the buckling load, corresponding to the values of K_x for which the eigenfrequencies vanish. It should be noted that for the ply-angles $\theta = 60^\circ$ and 90°, the minimum buckling loads correspond to $m = 2$ and $n = 1$, a fact that was clearly indicated in Fig. 12. From the point of view of buckling instability, the results obtained from this plot are in full agreement with those obtained in Ref. [12]. In the same context, the results of Fig. 13 reveal that when $L_R < 0$, i.e. in the case of tensile loads applied on edges $x_2 = 0_1, L_2$, there is a substantial increase of eigenfrequencies and of buckling loads, as compared to the case where $L_R \geqslant 0$.

One should also point out that the results based on the model of sandwich structures developed in this paper can be applied, as a special case, to symmetrically laminated anisotropic composite plates, for which an elegant solution of the free vibration and dynamic response was provided in Ref. [17].

8. Conclusions

An analytical study of the flexural free vibration behavior of flat sandwich panels featuring laminated anisotropic face sheets was presented. The closed-form solution obtained via implementation of the extended Galerkin solution methodology has enabled one to highlight the implications of a number of effects, such as orthotropicity ratio of the material of face sheets and core layer, ply-angle of the material of the faces, structural lay-up, panel aspect ratio and compressive/tensile edge loads. Moreover, the adopted solution methodology was validated against predictions obtained via experimental, analytical and numerical methods, and an excellent agreement was obtained. The results have revealed the considerable potentially beneficial role the directional property of face sheets material, transverse shear orthotropicity ratio of the core material and

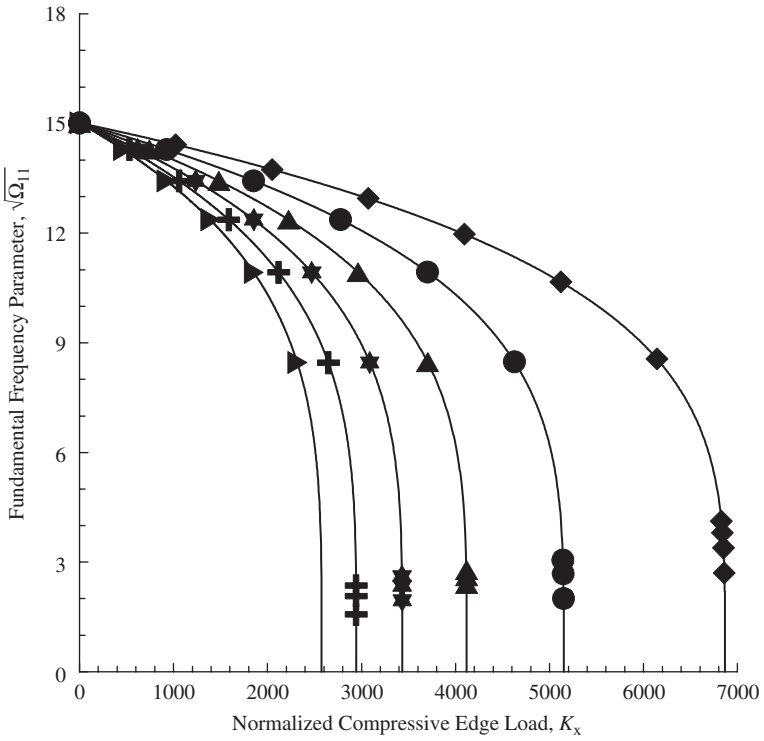

Fig. 13. Implications of biaxial tensile/compressive edge load on the fundamental dimensionless natural frequency $\Omega_{11}^{1/2}$, $\hat{h} = 0.02$ in. (0.508 mm), $\phi = 1$. The panel lay-up is $[45^\circ/-45^\circ/45^\circ/\text{core}/45^\circ/-45^\circ/45]$. (◆) $L_R = -0.25$; (●) $L_R = 0$; (▲) $L_R = 0.25$; (★) $L_R = 0.50$; (+) $L_R = 0.75$; (▶) $L_R = 1.0$.

the lay-up of the structure can play toward the enhancement, without weight penalties, of the vibrational behavior of sandwich panels.

Appendix

Expression of 2-D strain measures in terms of displacement quantities
For the bottom face sheets:

$$\begin{aligned}
&\varepsilon'_{11} = \eta_{1,1} + \zeta_{1,1} \quad (1 \rightleftarrows 2),\\
&\gamma'_{12} = \eta_{1,2} + \eta_{2,1} + \zeta_{1,2} + \zeta_{2,1},\\
&\kappa'_{11} = -v_{3,11} \quad (1 \rightleftarrows 2),\\
&\kappa'_{12} = -2v_{3,12}.
\end{aligned} \tag{A.1a–d}$$

In the core layer:

$$\bar{\gamma}_{13} = \frac{1}{\bar{h}}\left\{\eta_1 + \frac{1}{2}hv_{3,1}\right\} + v_{3,1} \quad (1 \rightleftarrows 2). \tag{A.2}$$

In the top face sheets:

$$\begin{aligned}
&\varepsilon''_{11} = \eta_{1,1} - \zeta_{1,1} \quad (1 \rightleftarrows 2),\\
&\gamma''_{12} = \eta_{1,2} + \eta_{2,1} - \zeta_{1,2} - \zeta_{2,1},\\
&\kappa''_{11} = -v_{3,11} \quad (1 \rightleftarrows 2),\\
&\kappa''_{12} = -2v_{3,12}.
\end{aligned} \tag{A.3a–d}$$

It should be remarked that the displacement measures ξ_α and η_α, as defined by Eqs. (3a,b), belong to the stretching and bending problems, respectively. As per the linear theory of symmetric sandwich flat panels, the governing equations involving ξ_α are decoupled from those expressed in terms of η_α and v_3. For the present problem, only the latter system of equations was considered.

References

[1] A.K. Noor, W.S. Burton, C.W. Bert, Computational models for sandwich plates and shells, *Applied Mechanics Reviews* 49 (1996) 155–199.

[2] D. Zenkert, *An Introduction to Sandwich Construction*, EMAS Publication, Chameleon Press LTD, London, UK, 1995.

[3] J.R. Vinson, *The Behavior of Sandwich Structures of Isotropic and Composite Materials*, Technomic Publications, Lancaster, PA, 1991.

[4] L. Librescu, T. Hause, Recent developments in the modeling and behavior of advanced sandwich constructions: a survey, *Journal of Composite Structures* 48 (1–3) (2000) 1–17.

[5] J.R. Vinson, Sandwich structures, *Applied Mechanics Reviews* 54 (2001) 201–214.

[6] J. Hohe, L. Librescu, Advances in the structural modeling and behavior of sandwich panels, *Mechanics of Advanced Materials and Structures* 11 (4–5) (2004) 395–424.

[7] L. Vu-Quoc, H. Deng, X.G. Tan, Geometrically exact sandwich shells: the dynamic case, *Computer Methods in Applied Mechanics and Engineering* 190 (2001) 2825–2873.

[8a] L. Vu-Quoc, X.G. Tan, Optimal solid shells for nonlinear analyses of multilayer composites statics, *Computer Methods in Applied Mechanics and Engineering, Part I* 192 (9–10) (2003) 975–1016.

[8b] L. Vu-Quoc, X.G. Tan, Optimal solid shells for nonlinear analyses of multilayer composites statics, *Computer Methods in Applied Mechanics and Engineering, Part II* 192 (9–10) (2003) 1017–1059.

[9] L. Vu-Quoc, I.K. Ebcioglu, On the physical meaning of the dynamical equations governing geometrically-exact multilayer shells, in: E. Ramm, W.A. Wall (Eds.), *Computer Methods in Applied Mechanics and Engineering*, *Computational Methods for Shells*, vol. 194(21–24), June 2005, pp. 2363–2384.

[10] L. Librescu, T. Hause, C.J. Camarda, Geometrically nonlinear theory of initially imperfect sandwich plates and shells incorporating non-classical effects, *AIAA Journal* 35 (8) (1997) 1393–1403.

[11] T. Hause, L. Librescu, T.F. Johnson, Thermomechanical load-carrying capacity of sandwich flat panels, *Journal of Thermal Stresses* 21 (6) (1998) 627–653.

[12] T. Hause, T.F. Johnson, L. Librescu, Effect of face-sheet anisotropy on buckling and postbuckling of flat sandwich panels, *Journal of Spacecraft and Rockets* 37 (3) (2000) 331–341.

[13] L. Librescu, *Elastostatics and Kinetics of Anisotropic and Heterogeneous Shell-type Structures*, Noordhoff International Publishing, Leyden, Netherlands, 1975.

[14] M.E. Raville, C.E.S. Ueng, Determination of natural frequencies of vibration of a sandwich plate, *Experimental Mechanics* 7 (1967) 490–493.

[15] G.R. Monforton, L.A. Schmidt Jr., Finite element analysis of sandwich plates and cylindrical shells with laminate faces, *Proceedings of Conference on Matrix Methods on Structural Mechanics* (1969) 573–616.

[16] H.B. Zhou, G.Y. Li, Free vibration analysis of sandwich with laminated faces using spline finite point method, *Computers and Structures* 59 (2) (1996) 257–263.

[17] A.L. Dobyns, Analysis of simply supported orthotropic subjected to static and dynamic loads, *AIAA Journal* 19 (5) (1981) 642–650.